

The Southern SHARC Survey: the $z = 0.3 - 0.7$ Cluster XLF¹

D.J. Burke^{2,3}, C.A. Collins³, R.M. Sharples², A.K. Romer^{4,6}, B.P. Holden⁵, R.C. Nichol⁶

ABSTRACT

We present the $z = 0.3-0.7$ cluster X-ray luminosity function (XLF) determined from the Southern SHARC (Serendipitous High-redshift Archival ROSAT Cluster) survey. Over the luminosity range $L \sim (0.3 - 3) \times 10^{44}$ erg s⁻¹ (0.5 - 2.0 keV) the XLF is in close agreement with that of the low redshift X-ray cluster population. This result greatly strengthens our previous claim of no evolution of the cluster population, at these luminosities, at a median redshift of $z = 0.44$.

Subject headings: galaxies: clusters: general — galaxies: evolution — X-rays: galaxies — X-rays: general

arXiv:astro-ph/9708145v1 15 Aug 1997

¹Based partly on data collected at the European Southern Observatory, La Silla, Chile, and the Anglo-Australian Telescope, Siding Spring, Australia

²Department of Physics, University of Durham, South Road, Durham DH1 3LE, UK

³Astrophysics Research Institute, School of Engineering, Liverpool John Moores University, Byrom Street, Liverpool L3 3AF, UK

⁴Department of Physics and Astronomy, Northwestern University, 2145 Sheridan Road, Evanston, IL 60208

⁵Department of Astronomy and Astrophysics, University of Chicago, 5640 S. Ellis Rd., Chicago, IL 60637

⁶Department of Physics, Carnegie Mellon University, 5000 Forbes Avenue, Pittsburgh, PA 15213-3890

1. Introduction

X-ray clusters of galaxies are efficient tracers of the mass in the Universe and can be studied out to large redshifts. Prior to the launch of the ROSAT X-ray telescope, the only high redshift ($z > 0.3$) X-ray selected cluster sample was that of the EINSTEIN Extended Medium Sensitivity Survey (EMSS; Henry et al. 1992; Gioia & Luppino 1994). Henry et al. (1992) used the EMSS to show X-ray clusters evolved ‘negatively’ — the space density of high luminosity clusters being lower in the redshift range $z = 0.30 - 0.60$ compared to $z = 0.14 - 0.20$. This result was in conflict with popular models of cluster formation (e.g. Kaiser 1986) and prompted further significant theoretical work (e.g. Kaiser 1991; Evrard & Henry 1991).

The maturing of the ROSAT database has sparked much recent interest in testing this result. A large cluster sample with a median depth of $z \sim 0.1$, created from the ROSAT All Sky Survey (RASS), shows no sign of evolution out to $z = 0.3$ (Ebeling et al. 1997). Castander et al. (1995) presented the first look at the high redshift cluster population with ROSAT, claiming that the evolution seen by Henry et al. (1992) extends to luminosities $\sim 10^{44}$ erg s $^{-1}$. We have recently shown (Collins et al. 1997), using the Southern SHARC⁷ sample of serendipitously detected clusters from deep ROSAT PSPC pointings, that the number of high redshift clusters is consistent with a no evolution model, in direct contrast to Castander et al. (1995). Finally, the EMSS sample has been re-analysed in the light of new optical and X-ray data, which indicates that the evidence for evolution seen by Henry et al. (1992) is not statistically significant (Nichol et al. 1997).

In this letter we present the high redshift X-ray luminosity function (XLF) of the Collins et al. (1997) cluster sample. In section 2 we describe the calculation of the XLF from this sample and in section 3 we discuss the results. Throughout this letter we have assumed $H_0 = 50$ km/s/Mpc and $q_0 = 0.5$ and quoted luminosities in the 0.5 to 2.0 keV pass band, unless explicitly stated otherwise.

2. Determination of the XLF

The cluster sample used in this letter is the Southern SHARC survey, consisting of 16 clusters in the redshift range $z = 0.3 - 0.7$ with a median redshift

of $z = 0.44$, detected in a serendipitous survey of 66 deep ROSAT PSPC pointings, covering a total search area of 17.7 deg 2 . This area is slightly larger than that used in Collins et al. (1997) due to the use of a different central source mask. Each pointing satisfies the following criteria: exposure time greater than 10 ks, $|b| > 20^\circ$, and $\delta < 20^\circ$. Further details of the sample are given in Collins et al. (1997) and a description of the full survey will be presented in a future paper.

For each cluster the count rate was measured from the background-subtracted count rate image in the 0.5 to 2.0 keV pass band. The chosen aperture encloses 80% of the light and was determined from a convolution of a King surface brightness profile with a model of the off-axis point spread function, using a cluster core radius of 250 kpc and $\beta = 2/3$ (Jones & Forman 1984). Justification for the adopted values of these cluster parameters is given below. After accounting for the flux falling outside this aperture, we used a thermal bremsstrahlung spectrum of temperature 6 keV (typical of nearby clusters) and a Galactic absorption model to convert the total count rate into a flux, and then into rest frame luminosities, L , in both the 0.5 to 2.0 keV and 0.3 to 3.5 keV pass bands. We chose to use a thermal bremsstrahlung model because cluster X-ray emission is dominated by the continuum radiation rather than line emission (e.g. Sarazin 1988) and for its computational ease of use. To investigate the uncertainty introduced by using a single temperature we have used a luminosity-temperature relation (Wang & Stocke 1993) to obtain iterated estimates of the cluster luminosities. These values are within 1% (0.5 - 2.0 keV) and 4% (0.3 - 3.5 keV) of those obtained above and the difference is negligible compared to the Poisson errors of the photon counts, which has a median value of 10%.

We have performed extensive simulations to model the effect of using an extent criterion to select cluster candidates. The ability to detect a given cluster depends on properties both intrinsic and extrinsic to the cluster — the relevant cluster characteristics are its luminosity, surface brightness profile and redshift; those for the survey are exposure time, background count rate and off-axis angle. The simulations assume a universal cluster X-ray surface brightness profile, namely the King model with a core radius of 250 kpc and $\beta = 2/3$ (Jones & Forman 1984), that is independent of redshift. Ideally one would use a distribution encompassing the true range of cluster profiles, however the sensitivity and spatial resolution of

⁷Serendipitous High-redshift Archival ROSAT Cluster

the current generation of X-ray instruments limit the knowledge of such a distribution to low redshift. Our choice of profile is consistent with the average properties of low redshift cluster samples (e.g. Henry et al. 1992; Jones & Forman 1984). As the simulations are computationally intensive we limited our analysis to a binned representation of the survey with regard to exposure time, background count rate and off-axis angle. The bin sizes were chosen so as to be small enough that the selection function did not vary significantly across a bin whilst being large enough that the simulations could be performed in a reasonable time. For each bin a range of cluster luminosities ($0.1 - 3.0 \times 10^{44}$ erg s $^{-1}$) and redshifts (0.2 – 0.9) were used; simulated clusters were generated by randomly distributing source photons using the King profile convolved with a model PSPC PSF and background photons using a flat background model. The number of source and background photons were Poisson distributed about the expected number.

Multiplying the selection function of a given bin by the survey area for the bin and summing over all the bins produces $\Omega(L, z)$, the available survey area as a function of cluster luminosity and redshift, shown in Figure 1. The survey volume for a cluster with luminosity L , in a redshift shell $z = z_1$ to z_2 , is $V_{\max}(L)$, defined as

$$V_{\max}(L) = \int_{z_1}^{z_2} \Omega(L, z) dV(z) dz, \quad (1)$$

where $dV(z)$ is the volume per square degree at a redshift z . Figure 2 shows equation (1) evaluated for the redshift shell $z = 0.3 - 0.7$ using the curves from Figure 1 where the solid line indicates the fit used to interpolate these points.

We have used both parametric and non-parametric forms to define the cluster XLF; a brief description follows and a full account of the fitting procedure can be found in Nichol et al. (1997). The non-parametric XLF, $n(L)$, was calculated using

$$n(L) = \sum_i \frac{1}{V_{\max}(L_i) \Delta L}, \quad (2)$$

where the sum is performed over all clusters whose luminosities, L_i , are within $\pm \Delta L/2$ of L . For a model XLF $\phi(L)$, the parametric form was determined by maximising the likelihood \mathcal{L} , given by

$$\mathcal{L} = \prod_i \frac{\int_0^\infty V_{\max}(L) \phi(L) E_i(L) dL}{\int_0^\infty V_{\max}(L) \phi(L) dL}, \quad (3)$$

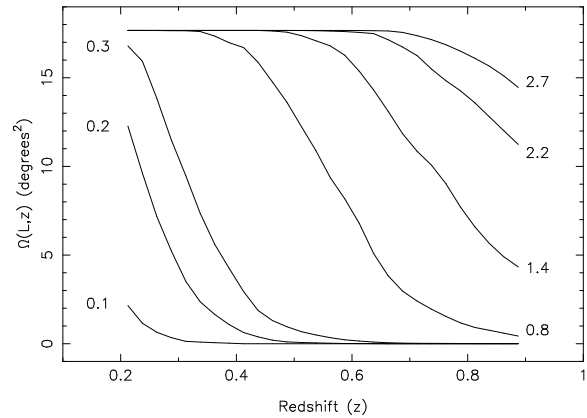


Fig. 1.— The available survey area, as a function of redshift, for the Southern SHARC survey. Each curve corresponds to a different cluster luminosity, labelled in units of 10^{44} erg s $^{-1}$, and was calculated using the simulations described in the text.

where the product is over the cluster detections and $E_i(L)$ is a normal distribution, with mean L_i and standard deviation equal to the error on L_i , which models the effect of luminosity errors on the fitting procedure.

In Figures 3 and 4 we show the non-parametric XLF, for the redshift shell $z = 0.3 - 0.7$, calculated using equations (1) and (2) for both the 0.5 - 2.0 keV and 0.3 - 3.5 keV pass bands. Table 1 lists the data points shown in these figures.

We fitted two parametric forms to the data: a power law (e.g. Henry et al. 1992),

$$\phi(L) = KL^{-\alpha}, \quad (4)$$

and a Schechter function (e.g. Ebeling et al. 1997),

$$\phi(L) = K_s \exp(-L/L_*) L^{-\alpha_s}. \quad (5)$$

As we are not sensitive to the characteristic luminosity, L_* , of the Schechter function, we used the best fit values from Ebeling et al. (1997) — 5.70×10^{44} erg s $^{-1}$ (0.5-2.0 keV) and 10.7×10^{44} erg s $^{-1}$ (0.3-3.5 keV). The likelihood for a given $\phi(L)$ is independent of the normalisation (K or K_s), so we fixed this by setting the expected number of clusters equal to the number in our sample. This procedure gives some weight to luminosities where no clusters were detected, producing a steeper slope than the non-parametric XLF would suggest (Henry et al. 1992). Errors on α and α_s were calculated by integrating the

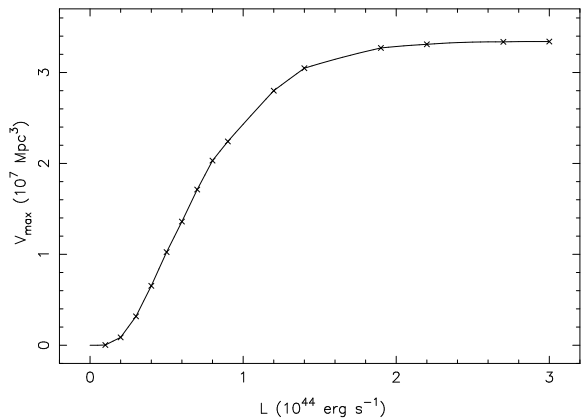


Fig. 2.— The symbols indicate the values of $V_{\max}(L)$, for the redshift shell $z = 0.3 - 0.7$, calculated using equation (1) and the curves shown in Figure 1. Luminosities are in units of $10^{44} \text{ erg s}^{-1}$ and the solid curve is the fit to these points.

normalised likelihood distributions, which are well approximated by a Gaussian, out to an enclosed area of 68.3% and those for the normalisations were found by allowing α to take its one-sigma values. The results are listed in Table 2 and shown graphically in Figures 3 and 4.

3. Discussion

From Figure 3 it is qualitatively obvious that, for $L \sim 10^{44} \text{ erg s}^{-1}$, our $z = 0.3 - 0.7$ cluster XLF is consistent with that of the low redshift cluster XLF. Our best fit faint end slope for the Schechter function, $\alpha_s = 1.77 \pm 0.30$, agrees with that of the low redshift cluster sample of Ebeling et al. (1997), who find $\alpha_s = 1.85 \pm 0.09$. The power-law slope in the EMSS pass band ($\alpha = 2.22 \pm 0.25$) is also consistent with the slope of the low redshift shell of Henry et al. (1992) and the re-worked EMSS sample of Nichol et al. (1997), for which $\alpha = 2.19 \pm 0.21$ and $\alpha = 2.60 \pm 0.37$ respectively. The lack of luminosity evolution agrees with our recent analysis of the redshift distribution of the Southern SHARC clusters (Collins et al. 1997) and is inconsistent with the strong evolution claimed by Castander et al. (1995). Our results strengthen, and extend to higher redshift, recent claims that cluster properties remain the same out to $z \simeq 0.3$ (e.g. Ebeling et al. 1997; Mushotzky & Scharf 1997).

The only other published XLF for X-ray selected

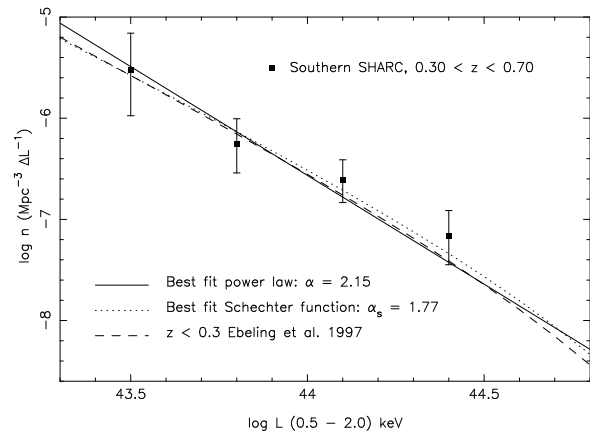


Fig. 3.— The XLF of the Southern SHARC in the 0.5 to 2.0 keV pass band. The solid line is our best power-law fit, the dotted line our best fit Schechter function and the dashed line is the Schechter function fit of Ebeling et al. (1997) to their low redshift RASS cluster sample.

clusters covering our redshift range is that of Henry et al. (1992) from 21 EMSS clusters between $z = 0.3 - 0.6$, with a median redshift of 0.33. They find a much steeper power-law slope of $\alpha = 3.27 \pm 0.29$, which they claim is the result of negative evolution. Our XLF is consistent with the non-parametric XLF of Henry et al. (1992) for luminosities $\lesssim 5 \times 10^{44} \text{ erg s}^{-1}$ (0.3 - 3.5 keV), as shown in Figure 4, hence any evolution of the cluster population is restricted to luminosities $\gtrsim 3 \times 10^{44} \text{ erg s}^{-1}$. Using the Ebeling et al. (1997) XLF, and assuming 100% detection efficiency, we find that the surface density of clusters with $L > 3 \times 10^{44} \text{ erg s}^{-1}$, in the redshift range 0.3 to 0.7, is 0.083 deg^{-2} and the expected number of such clusters in the Southern SHARC survey is only ~ 1.5 . Therefore the lack of high luminosity clusters in our sample is not unexpected. In Figure 4, we plot equation (6) of Henry et al. (1992) using their best-fit values of $n = -2.10$ and $k_0 = 0.029h \text{ Mpc}^{-1}$, for $z = 0.37$, corresponding to the median redshift of the joint cluster sample. This analytical model is based on the Press-Schechter formalism and is shown here simply to provide a physical basis for extrapolating the EMSS data and comparing the two samples. In the context of general cluster formation theories, our result is broadly consistent with the predictions of entropy-based models or a low value of the density parameter (e.g. Kaiser 1991; Evrard & Henry 1991; Henry et al. 1992; Oukbir & Blanchard 1997; Bower

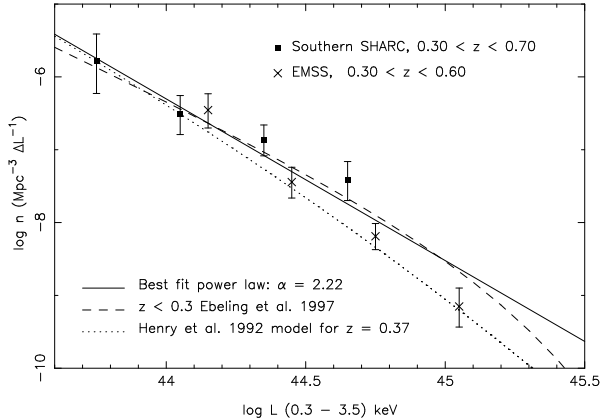


Fig. 4.— The solid points show the Southern SHARC XLF in the 0.3 to 3.5 keV pass band and the solid line is our best power-law fit. The crosses indicate the high redshift XLF from Henry et al. (1992) with the dotted line showing their best fit model ($n = -2.10$, $k_0 = 0.029h \text{ Mpc}^{-1}$) evaluated at a redshift of 0.37, the median of the combined cluster sample. The dashed line is the Schechter function fit of Ebeling et al. (1997).

1997; Mathiesen & Evrard 1997).

4. Conclusion

We have used the Southern SHARC survey to create the first $z > 0.3$ XLF derived from ROSAT detected clusters of galaxies. Comparison with the low redshift cluster XLF of both ROSAT (Ebeling et al. 1997) and EMSS (Henry et al. 1992) clusters shows that there is no evolution in the X-ray luminosities of $L \sim 10^{44} \text{ erg s}^{-1}$ clusters at a median depth of $z = 0.44$. This is consistent with our analysis of the redshift distribution of this cluster sample (Collins et al. 1997) and adds further weight to the body of evidence for no evolution in the cluster population.

This research has made use of data obtained from the Leicester Database and Archive Service at the Department of Physics and Astronomy, Leicester University, UK. DJB acknowledges PPARC for a Postgraduate Studentship and PDRA, CAC acknowledge PPARC for an Advanced Fellowship, AKR acknowledges support from NASA ADP grant NAG5-2432, and BH acknowledges support by the Center for Astrophysical Research in Antarctica (NSF OPP 89-20223).

REFERENCES

- Bower, R. G. 1997, MNRAS, in press, astro-ph/9701014
 Castander, F. J., et al. 1995, Nature, 377, 39
 Collins, C. A., Burke, D. J., Romer, A. K., Sharples, R. M., & Nichol, R. C. 1997, ApJ, 479, L117
 Ebeling, H., Edge, A. C., Fabian, A. C., Allen, S. W., Crawford, C. S., & Böhringer, H. 1997, ApJ, 479, L101
 Evrard, A. E., & Henry, J. P. 1991, ApJ, 383, 95
 Gehrels, A. 1986, ApJ, 303, 336
 Gioia, I. M., & Luppino, G. A. 1994, ApJS, 94, 583
 Henry, J. P., Gioia, I. M., Maccacaro, T., Morris, S. L., Stocke, J. T., Wolter, A. 1992, ApJ, 386, 408
 Jones, C. & Forman, W. 1984, ApJ, 276, 38
 Kaiser, N. 1986, MNRAS, 222, 323
 Kaiser, N. 1991, ApJ, 383, 104
 Mathiesen, B., & Evrard, A. E. 1997, MNRAS, submitted, astro-ph/9703176
 Mushotzky, R. F., & Scharf, C. A. 1997, ApJ, 482, L13
 Nichol, R. C., Holden, B. P., Romer, A. K., Ulmer, M. P., Burke, D. J., & Collins, C. A. 1997, ApJ, 481, 644
 Oukbir, J., & Blanchard, A. 1997, A&A, 317, 1
 Sarazin, C. L. 1988, X-ray emission from clusters of galaxies (Cambridge: Cambridge University Press)
 Wang, Q., & Stocke, J. T. 1993, ApJ, 408, 71

This 2-column preprint was prepared with the AAS L^AT_EX macros v4.0.

TABLE 1
THE NON-PARAMETRIC XLF FOR THE SOUTHERN SHARC SURVEY.

pass band (keV)	$\log L^a$	$\log n(L)^b$
0.5 – 2.0	43.50	-5.52 (+0.37, -0.45)
0.5 – 2.0	43.80	-6.26 (+0.25, -0.28)
0.5 – 2.0	44.10	-6.61 (+0.20, -0.22)
0.5 – 2.0	44.40	-7.17 (+0.25, -0.28)
0.3 – 3.5	43.75	-5.78 (+0.37, -0.45)
0.3 – 3.5	44.05	-6.51 (+0.25, -0.28)
0.3 – 3.5	44.35	-6.86 (+0.20, -0.22)
0.3 – 3.5	44.65	-7.42 (+0.25, -0.28)

^a L has units of erg s^{-1}

^b $n(L)$ has units of $\text{Mpc}^{-3} \Delta L^{-1}$

NOTE.— Luminosity bins have a constant width and were chosen so that each bin contained at least two clusters. Poisson errors (one-sigma) are from Gehrels (1986).

TABLE 2
THE PARAMETRIC XLF FOR THE SOUTHERN SHARC SURVEY.

pass band (keV)	α	K^a	α_s	K_s^a
0.5 - 2.0	2.15 ± 0.23	2.72 ± 0.12	1.77 ± 0.30	3.64 ± 0.16
0.3 - 3.5	2.22 ± 0.25	4.99 ± 0.77	1.78 ± 0.30	5.68 ± 1.04

^aUnits of $10^{-7} \text{Mpc}^{-3} (10^{44} \text{erg s}^{-1})^{\alpha-1}$